New theories of α-radioactivity

P.O.G. Ogunbade* **and S.A. Rakityansky*‡**

We review the radioactive decay of nuclei via emission of α-particles using three different theoretical approaches. The half-lives of the radioactive nuclei, calculated using these three methods, are compared with each other and with available experimental data. The results show that the superasymmetric fission model with the double-folding procedure for obtaining the α-nucleus potential is the most reliable among the three models studied.

Introduction

The problem of α-decay is even older than nuclear physics itself. More than a century has passed since the discovery of radioactivity. The first qualitative interpretation of α-decay was given in the early 1920s in terms of tunnelling through a quantum-mechanical potential barrier.[1,2] Numerous experimental facts have been acquired since then, and many theoretical approaches developed. Modern theories are able accurately to reproduce the relative half-lives for a wide range of radioactive isotopes. It is, however, far more difficult to account for their absolute values. Nowadays, experimentalists continue to measure half-lives using constantly improving techniques, and theoreticians pursue their quest for an adequate theory of α-decay.

The process of α-decay can be described in terms of a quantum-mechanical decaying state,[3] in which α-cluster formation and barrier penetration are contingencies inherent to a quasi-stationary state, or as a superasymmetric fission that may be visualized as a sequence of adiabatic rearrangements, i.e. as a continuous change of variables.[4] About twelve years ago, two theoretically 'extreme' approaches were developed based on these ideas: the cluster-like and the fission-like theories.[5] In the cluster approach the α-emission is treated in a natural way, whereas in the fission model the α-decay process is considered as a very asymmetric fragmentation of the parent nucleus. The main difference between these two models consists in the behaviour of the system before the formation of the nascent fragments. In both approaches, however, the potential barriers are identical beyond the touching distance between the separating fragments.

The physics of the α-decay is comprehensively described in the papers by Buck *et al.*[6–9] and in a number of other systematic studies.[11,12] Recently, new measurements and improved models of the α-decay have been reported.[13–16] In particular, a new approach proposed in ref. 13 uses the fact that a narrow resonance behaves almost like a bound state with real energy. Its wave function has a strongly decreasing behaviour inside the barrier and can be normalized to unity in the internal region. To ensure the continuity, the external outgoing spherical Coulomb wave should be multiplied by some coefficient. This matching coefficient squared is proportional to the decay width, that is, to the inverse half-life.

The main objective of our work is to test and discuss the reliability of three different theoretical approaches: the quasi-stationary decaying state approach, the superasymmetric fission model, and the simple quasi-classical description of the barrier penetration. The nuclear potentials we need for both the superasymmetric fission and quasi-classical models are obtained microscopically by folding the realistic M3Y effective interaction with the nuclear density distributions of the two fragments.

Decay theories

Alpha emitters can be treated as extremely narrow quantum resonances, that is, isolated quasi-stationary states. To describe their structure, we use the fact that a narrow resonance behaves almost like a bound state with real energy.

In the usual microscopic approach, the calculation of the decay width requires knowledge of the initial and final state wave functions and the interaction potential. In principle, the potential $V_{\alpha\mathrm{A}}$ should consist of a sum of two-body terms describing the pairwise interactions between the outgoing α particle and all nucleons in the daughter nucleus. As is often done, however, the 'true' many-body interaction $V_{\alpha\mathrm{A}}$ is approximated by the much simpler two-body α-nucleus potential

$$V(r) = V_N(r) + V_C(r) + V_\ell \ , \tag{1}$$

which is the sum of the nuclear V_N, the Coulomb V_C, and the centrifugal

$$V_\ell = \frac{\hbar^2}{2\mu}\frac{\ell(\ell+1)}{r^2}$$

terms, where $\mu = mA_\alpha A_d/A$ is the reduced mass with A, A_d, and A_α being the mass numbers of the parent, the daughter, and the α nuclei, respectively, and m the nucleon mass. The angular momentum ℓ determining the lowest possible centrifugal barrier is obtained from the spin-parity conservation law.

For the Coulomb interaction V_C in Equation (1), we assume that the α particle is a point-like charge and the daughter nucleus has a uniform spherical charge distribution (SCD) with radius R_c, hence

$$\begin{aligned} V_C(r) &= \frac{Z_\alpha Z_d e^2}{r} \ , && \text{for } (r \geq R_c), \\ &= \frac{Z_\alpha Z_d e^2}{2R_c}\left[3 - \left(\frac{r}{R_c}\right)^2\right] \ , && \text{for } (r \leq R_c) \ , \end{aligned} \tag{2}$$

where Z_α and Z_d are the charges of the α particle and the core, respectively.

Once the decay width Γ is calculated, the corresponding half-life is obtained as

$$T_{1/2} = \frac{\hbar}{\Gamma}\ln 2 \ . \tag{3}$$

Experimental values of $T_{1/2}$ for different nuclei vary over a very wide range: $\sim 10^{-6}$–10^{22} s. As mentioned above, most of the α-nucleus resonances are long-lived, i.e. extremely narrow, which makes it difficult numerically to locate the corresponding S-matrix poles.

The three methods for calculating Γ, which we test in the present paper, are described next.

The quasi-stationary decaying state approach

Within the standard microscopic approach, the α-decay width

*Physics Department, University of South Africa, P.O. Box 392, Pretoria 0003, South Africa.
‡Author for correspondence. E-mail: rakitsa@science.unisa.ac.za

for spherical nuclei is calculated as follows (see, for example, refs 3, 17).

$$\Gamma \equiv \sum_{\ell} \Gamma_{\ell} = \lim_{r\to\infty} \hbar v \sum_{\ell} |g_{\ell}(r)|^2 \ , \tag{4}$$

where v is the α-particle velocity relative to the emitter, and $g_\ell(r)$ is the radial component of the wave function describing their relative motion. In the external region, beyond the touching configuration, the function g_ℓ obeys the Schrödinger equation

$$\left[\frac{d^2}{dr^2} + k^2 - \frac{\ell(\ell+1)}{r^2} - U(r)\right] g_{\ell}(r) = 0 \ , \tag{5}$$

where $U(r) = (2\mu/\hbar^2)V(r)$ and $k^2 = (2\mu/\hbar^2)E$. Far away from the emitter, where $V(r)$ becomes a purely Coulomb potential, the solution of Equation (5) is a Coulombic spherical outgoing wave

$$g_{\ell}(r) \underset{r\to\infty}{\longrightarrow} C_{\ell}[G_{\ell}(\eta, kr) + iF_{\ell}(\eta, kr)] \ , \tag{6}$$

where F_ℓ and G_ℓ are the standard regular and irregular Coulomb functions and η is the Sommerfeld parameter. Since $\lim_{r\to\infty}|G_\ell(\eta, kr) + iF_\ell(\eta, kr)| = 1$, the partial decay width is proportional to the normalization coefficient squared, i.e.

$$\Gamma_{\ell} = \hbar v\, |C_{\ell}|^2 \ . \tag{7}$$

In order to determine C_ℓ, the Schrödinger equation (5) is solved backwards starting from a far-away point with the asymptotic condition (6), where for C_ℓ an arbitrary number is chosen, say, $C_\ell = 1$. When the point $r = R$ separating the internal and external regions is reached, the thus calculated function $g_\ell(r)$ is renormalized to match a resonant state solution $\phi_{n\ell j}(r)$ in the internal region. The function $\phi_{n\ell j}(r)$ obeys the same Schrödinger equation (5) with the conditions

$$\phi_{n\ell j}(r) \underset{r\to 0}{\longrightarrow} 0 \ , \quad \phi_{n\ell j}(r) \underset{r\to\infty}{\longrightarrow} G_{\ell}(\eta, kr) \ ,$$

and has n nodes in the internal region. The matching of the two solutions thus gives

$$\Gamma_{\ell} = \hbar v \frac{\phi^2_{n\ell j}(R)}{G^2_{\ell}(\eta, kR) + F^2_{\ell}(\eta, kR)} \ .$$

Since $F_\ell(\eta, kr) \ll G_\ell(\eta, kr)$ inside the barrier, further approximation is justified, namely,

$$\Gamma_{\ell} = \hbar v \left[\frac{\phi_{n\ell j}(R)}{G_{\ell}(\eta, kR)}\right]^2 \ . \tag{8}$$

In what follows, the quasi-stationary decaying state approach will be referred to as Method A.

The superasymmetric fission model

In the superasymmetric fission model (SAFM), the formation of an α cluster is part of the deformation process. It is assumed that the remaining core and the cluster have spherical shapes and the α cluster gradually sticks out of the core nucleus. The potential energy of the system depends on the deformation parameter, which is the separation between the fragment centres. The fragments vibrate along the deformation line with the energy E_v that determines the so-called assault frequency $\nu = E_v/h$, i.e. the number of attempts to break away through the barrier. The zero-point vibration energy E_v can be determined using a model that describes the collective motion responsible for the superasymmetric deformation.

The half-life $T_{1/2}$ of the parent nucleus against its split into an α-particle and a daughter nucleus is calculated in the superasymmetric fission model as (see ref. 16),

$$T_{1/2} = \frac{h \ln 2}{2E_v}(1 + e^K) \ , \tag{9}$$

where K is the action integral

$$K = \frac{2}{\hbar}\int_{r_a}^{r_b} \{2\mu[V(r) - E_v - Q_{\alpha}]\}^{1/2}\, dr \ . \tag{10}$$

The Q_α term is the energy released in the decay process, the so-called Q-value. It can be obtained either from the kinetic energy of the α particle (corrected for the recoil) or from the binding energies of the parent and daughter nuclei.

For a parent nucleus with even N and even Z, the value of E_v is $0.1045Q_\alpha$ and when N is odd while Z even, $E_v = 0.0907Q_\alpha$.[18] The r_a and r_b terms are the inner and outer turning points of the barrier, determined from the equation

$$V(r) - E_v - Q_{\alpha} = 0 \ .$$

In this paper, we refer to this approach as Method B.

The quasi-classical method

The quasi-classical (or WKB) method is based on the calculation of the penetration probability for the α particle moving through the potential barrier. The α cluster is assumed to be formed inside the parent nucleus with certain preformation probability P.

The WKB method is expected to be a good approximation for low-lying metastable states. The quasi-classical expressions for Γ can be derived using the two-potential approach.[19,20] The resulting decay width is written as

$$\Gamma = PF\frac{\hbar^2}{4\mu}\exp\left[-2\int_{r_2}^{r_3} k(r)\, dr\right] \ , \tag{11}$$

where

$$\hbar k(r) = \sqrt{2\mu|E - V(r)|} \tag{12}$$

is the classical momentum, r_i ($i = 1, 2, 3$) are the classical turning points, and $E = Q_\alpha$. The normalization factor F is determined from the equation

$$F\int_{r_1}^{r_2} dr \frac{1}{k(r)}\cos^2\left(\int_{r_1}^{r} dr' k(r') - \frac{\pi}{4}\right) = 1 \ ,$$

where the squared cosine factor may be replaced with 1/2 without significant loss of accuracy, so that

$$F\int_{r_1}^{r_2} \frac{dr}{2k(r)} = 1 \ .$$

It should be pointed out that the preformation factor P must be smaller than 1, otherwise, as in the simple two-body model, we would assume that the ground state wave function of the parent nucleus contains a pure α-daughter configuration. The decay width in such a model would always overestimate the experimental decay width. We determine the preformation factor P from the ratio of the calculated to the measured half-lives.[16] The WKB approximation shall be referred to in this paper as Method C.

α-nucleus interaction potential

There is clear proof that the wavefunction of an α-radioactive nucleus has a non-negligible component corresponding to the configuration in which the α cluster is present.[22,23,34] After the decay, the α particle is in the scattering state relative to the daughter nucleus. Therefore, an effective α-nucleus potential should describe simultaneously the half-life of the α emitter and the elastic scattering of the α particle from the daughter nucleus.

The α-nucleus potentials available in the literature are constructed using two different approaches. The first of them is

based on a phenomenological optical model, while in the second the α-nucleus potential is viewed as the sum of individual *NN*-potentials, which means that this is a microscopic approach.

In the optical model, the αA-potential is usually approximated by a Woods-Saxon (WS) curve. This potential is real because no absorption processes are involved in the α-decay. Only the central term is considered and is given by

$$V(r) = \frac{V_0}{1 + \exp[(r - R_0)/a]} \ , \qquad (13)$$

with $R_0 = r_0 A^{1/3}$, where A is the mass number of the daughter nucleus. For fixed r_0 and the diffuseness parameter α (see, for example, refs 24, 25), the depth V_0 is adjusted so that the ground-state energy $E = -Q_\alpha$ is reproduced. The optical model therefore involves at least one fitting parameter, which makes it somewhat phenomenological and reduces its predictive power.

In the present paper, we follow a microscopic (*ab initio*) approach which is free from fitting parameters. Among the microscopic theories, the most popular is the double-folding (DF) model.[22,26] Starting from a two-body *NN*-potential V_{NN} and the nuclear densities ρ_1 and ρ_2 of the α-particle and the daughter nucleus, the αA-potential is constructed as the following integral

$$V_{\alpha A}(R) = \iint \rho_1(\vec{r}_1)\rho_2(\vec{r}_2)V_{NN}(|\vec{r}_2 - \vec{r}_1 + \vec{R}|, \rho_1, \rho_2, E)\, d\vec{r}_1\, d\vec{r}_2 \ , \quad (14)$$

where, besides the configuration vectors shown in Fig. 1, the *NN* potential (in general) depends on the nuclear densities and the collision energy E. In principle, the DF potential should contain both the direct and the nucleon exchange terms. However, the latter is considerably more difficult to handle in practice. Thus, for some applications, the single-nucleon exchange term is simulated by a delta function pseudopotential.[27] It can also be taken into account via introducing the energy and density dependence of the two-body interaction. This is why the potential V_{NN} in Equation (14) depends on ρ_1, ρ_2, and E.

In our work, we use the density-dependent (but E-independent) *NN*-interaction, namely, the so-called DDM3Y potential,[28,29]

$$V_{NN}(s, \rho_1, \rho_2, E) = \left(7999\frac{e^{-4.0s}}{4.0s} - 2134\frac{e^{-2.5s}}{2.5s} - 276\delta(s)\right) t(\rho_1, \rho_2)$$

with

$$t(\rho_1, \rho_2) = (1 - \beta\rho_1^{2/3})(1 - \beta\rho_2^{2/3}) \ ,$$

where the depth parameters are in MeV, distances in fm, and β = 1.6 fm^3. The ρ_1 and ρ_2 terms in our calculations are modelled as suggested in refs 27, 29, 30. The α-particle density is assumed to be of Gaussian form,

$$\rho_1(r) = 0.4229 \exp(-0.7024 r^2) \ , \qquad (15)$$

while the density distributions of the daughter nuclei are chosen to be of the spherically symmetric Woods-Saxon form,

$$\rho_2(r) = \frac{\rho_0}{1 + \exp[(r - c)/a]} \ , \qquad (16)$$

where

$$c = r_\rho(1 - \pi^2 a^2/3r_\rho^2), \quad r_\rho = 1.13A^{1/3}, \quad \text{and} \quad a = 0.54\,\text{fm} \ ,$$

and the value of ρ_0 is fixed by equating the volume integral of the density function to the mass number A of the residual daughter nucleus.

In the present work, the double-folding potential is calculated using the computer code DFPOT.[31] For the Coulomb part of the interaction, we use Equation (2) with $R_c = 1.3A^{1/3}$ (fm).

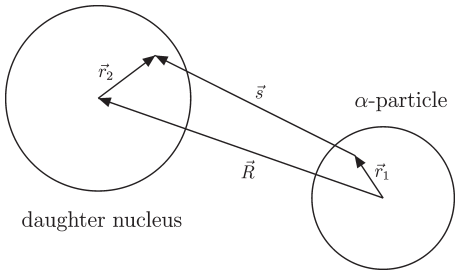

Fig. 1. Vectors used in the double-folding integral (14).

Results and discussion

To avoid unnecessary complications, we consider only nuclei which decay to the daughter ground state with 100% probability and for which the spins of both the initial and final states are known.The masses of the nuclear ground states, needed for determining the Q-values, are taken from the mass excess table of ref. 32.

We did the calculations for a wide range of α-decaying nuclei, using the three theoretical methods. The half-lives thus obtained are presented in Table 1. For all the 16 nuclei we consider, the calculations reproduce the experimental half-lives (taken from ref. 16) to within a factor of 12 or better.The only exceptions are the nuclei ^{208}Po and ^{217}Th, for which the effects of the proton and neutron shell closure make it difficult to achieve good accuracy with the simple potential.[6,7] Comparing the values of $T_{1/2}$ presented in Table 1, we see that all three methods we tested give similar results. Therefore, if one is satisfied with an order-of-magnitude estimate, the simplest, Method C, is an appropriate tool. The half-lives obtained with Method A differ from those from Method B not more than in 10%. Method C gives half-lives that are practically identical to those obtained with Method B.

Method C slightly over-estimates the half-lives.The reason for this is that it completely neglects the parent nucleus configuration in which the α-particle is dissolved among other nucleons. Despite this, the general trend of the half-lives calculated using Method C is rather good. The more sophisticated Method B takes into account the processes of the α-cluster dissociation. It is not unexpected, therefore, that it gives a better agreement with the experimental half-lives.

Figure 2 graphically compares the half-lives obtained with the different models, with the corresponding measured values. For the neutron-deficient nuclei, all three methods agree with each other and the observed values. The discrepancy among the

Table 1. Experimental $T_{1/2}^{\text{exp}}$ and calculated $T_{1/2}^{\text{calc}}$ half-lives of the α emitters.

Nucleus		$T_{1/2}^{\text{calc}}$ (s)			$T_{1/2}^{\text{exp}}$ (s)
	Q (MeV)	A	B	C	
^{144}Nd	1.905	1.541×10^{22}	8.383×10^{21}	8.423×10^{22}	7.219×10^{22}
^{146}Sm	2.529	3.495×10^{14}	3.619×10^{14}	2.768×10^{15}	3.248×10^{15}
^{150}Gd	2.809	6.603×10^{12}	8.210×10^{12}	5.326×10^{13}	5.646×10^{13}
^{152}Gd	2.205	5.545×10^{20}	3.946×10^{20}	4.065×10^{21}	3.406×10^{21}
^{174}Hf	2.495	6.347×10^{22}	7.480×10^{22}	3.344×10^{23}	6.307×10^{22}
^{190}Pt	3.250	5.025×10^{17}	1.095×10^{18}	2.146×10^{19}	2.050×10^{19}
^{208}Po	8.954	1.138×10^{-8}	9.849×10^{-8}	2.895×10^{-7}	2.990×10^{-7}
^{212}Po	5.216	7.056×10^{5}	4.066×10^{6}	5.954×10^{7}	9.139×10^{7}
^{216}Rn	8.200	3.461×10^{-6}	4.495×10^{-5}	8.881×10^{-5}	4.500×10^{-5}
^{217}Th	9.424	3.027×10^{-3}	2.054×10^{-5}	1.429×10^{-4}	2.520×10^{-4}
^{224}Ra	5.789	2.538×10^{4}	2.638×10^{5}	9.468×10^{5}	3.162×10^{5}
^{227}Ac	5.042	1.878×10^{9}	2.102×10^{10}	9.780×10^{10}	4.975×10^{10}
^{229}U	6.475	1.437×10^{3}	1.266×10^{4}	4.979×10^{4}	1.740×10^{4}
^{232}Th	4.083	6.557×10^{16}	3.955×10^{17}	2.509×10^{18}	4.431×10^{17}
^{240}Cm	6.397	1.094×10^{5}	1.575×10^{6}	7.733×10^{6}	2.345×10^{6}
^{256}Fm	7.027	5.687×10^{3}	1.094×10^{5}	4.650×10^{5}	1.167×10^{5}

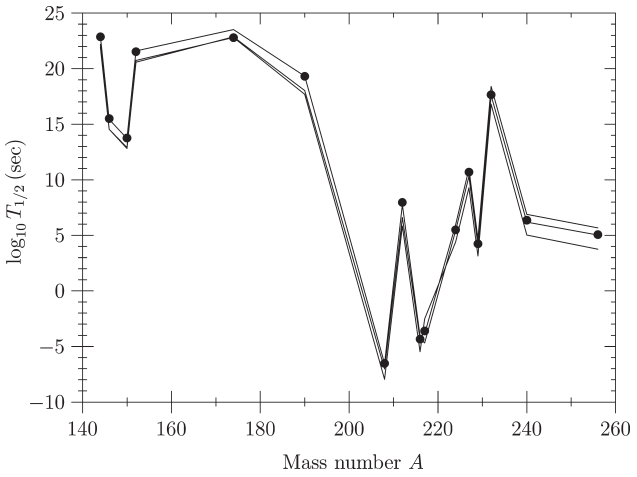

Fig. 2. The calculated (lines) and measured (circles) half-lives of 16 α-radioactive nuclei as functions of the atomic mass number. Their numerical values are given in Table 1.

models is seen for the nucleon number A within the interval from ∼170 to ∼210.

Conclusion

In this paper, we compare three different theories describing the ground-state alpha radioactivity of spherical nuclei: the quasi-bound state wavefunction approach, the superasymmetric fission model, and the quasi-classical method. Although these models have different degrees of sophistication, they nonetheless give rather similar results. The physical feature of the decay process, which is common to all three models, is the motion of the α-cluster through the barrier. The agreement among the models means that this feature is fundamental. Therefore, any model based on the concept of relative α-core motion should give at least a correct order of magnitude for the half-life.

An important part of the models considered in this paper is the α-nucleus potential. The calculations were done using an *ab initio* microscopic potential. With such an approach, the α-nucleas interaction is treated adequately. Indeed, ref. 33 shows that a systematic double-folding potential is able to reproduce both the elastic α scattering from the core-nucleus and the bound-state properties of the corresponding compound nuclear system.

It is worth mentioning that our calculations with the microscopic potential were done without adjusting any parameters. Despite this, the half-lives, ranging from 10^{-7} s to 10^{22} s, were reproduced equally well. Refinements such as an introduction of dissipation while tunnelling through the barrier, may further improve the results. Such calculations could be used, for example, to estimate the lifetimes of some exotic nuclei.

One of us (P.O.G.O.) wishes to express his gratitude to the University of South Africa for financial support, and to acknowledge fruitful discussions with B.N. Basu.

Received 12 December 2005. Accepted 5 January 2007.

1. Gamow G. (1928). Zur Quantentheorie des Atomkernes. *Z. Phys.* **51**, 204–212.
2. Condon E.U. and Guerney R.W. (1929). Quantum mechanics and radioactive disintegration. *Phys. Rev.* **33**, 127–140.
3. Mang H.J. (1964). Alpha decay. *Ann. Rev. Nucl. Sci.* **14**, 1–28.
4. Greiner W., Ivassscu M., Poenaru D. N and Sauaundulescu A. (1989). Cluster radioactivity. In *Treatise on Heavy Ion Science,* vol. 8., ed. D.A. Bromley, pp. 641–722. Plenum, New York.
5. Sauaundulescu A. and Greiner W. (1992). Cluster decay. *Rep. Prog. Phys.* **55**, 1423–1481.
6. Buck B., Merchant A.C. and Perez S.M. (1990). New look at α decay of heavy nuclei. *Phys. Rev. Lett.* **65**, 2975–2977.
7. Buck B., Merchant A.C. and Perez S.M. (1991). Groundstate to ground state alpha decays of heavy even-even nuclei. *J. Phys. G: Nucl. Part. Phys.* **17**, 1223–1235.
8. Buck B., Merchant A.C. and Perez S.M. (1992). α decay calculations with a realistic potential. *Phys. Rev. C* **45**, 2247–2253.
9. Buck B., Merchant A.C. and Perez S.M. (1993). Half-lives of favored alpha decays from nuclear ground states. *At. Data Nucl. Data Tables* **54**, 53–73.
10. Buck B., Merchant A.C. and Perez S.M. (1995). Systematics of alpha-cluster states above double shell closures. *Phys. Rev. C* **51**, 559–565.
11. Brown B.A. (1992). Simple relation for alpha decay half-lives. *Phys. Rev. C* **46**, 811–814.
12. Poenaru D.N. and Ivascu D. (1983). Estimation of the alpha decay half-lives. *J. Physique* **44**, 791–796.
13. Delion D.S. and Sauaundulescu A. (2002). Towards a self-consistent microscopic α-decay theory. *J. Phys. G: Nucl. Part. Phys.* **28**, 617–625.
14. Delion D.S. and Liotta R.J. (1998). Microscopic description of α-decay from super deformed nuclei. *Phys. Rev. C* **58**, 2073–2080.
15. Delion D.S., Insolia A. and Liotta R.J. (1996). New single particle basis for microscopic description of decay processes. *Phys. Rev. C* **54**, 292–301.
16. Poenaru D.N., Schnabel D., Greiner W., Mazilu D. and Gherghescu R. (1991). Nuclear lifetimes for cluster radioactivities. *At. Data Nucl. Tables* **48**, 231–327.
17. Lovas R.G., Loitta R.J., Insolia A., Varga K. and Delion D.S. (1998). Microscopic theory of cluster radioactivity. *Phys. Rep.* **294**, 265–362.
18. Poenaru D.N., Greiner W., Depta K., Ivauauscu M., Mazilu D and Sandulescu A. (1986). Calculated half-lives and kinetic energies for spontaneous emission of heavy ions from nuclei. *At. Data Nucl. Tables* **34**, 423–538.
19. Gurvitz S.A. and Kalbermann G. (1987). Decay width and shift of a quasi-stationary state. *Phys. Rev. Lett.* **59**, 262–265.
20. Gurvitz S.A. (1988). Novel approach to tunnelling problems. *Phys. Rev. A* 3**8**, 1747–1759.
21. Arima A. and Yoshida S (1974). Analysis of α-decay widths of light 4n nuclei. *Nucl. Phys. A* **219**, 475–515.
22. Satchler G.R. and Love W.G. (1979). Folding model potentials from realistic interactions for heavy-ion scattering. *Phys. Rep.* **55** 183–254.
23. Kobos A.M., Brown B.A., Lindsay R. and Satchler G.R. (1984). Folding model analysis of elastic and inelastic α-particle scattering using a density-dependent force. *Nucl. Phys. A* **425**, 205–232.
24. Harada K. and Rauscher E.A. (1968). Unified theory of alpha decay. *Phys. Rev.* **169**, 818–824.
25. McFadden L. and Satchler G.R. (1966). Optical-model analysis of the scattering of 24.7 MeV alpha particles. *Nucl. Phys.* **84**, 177–200.
26. Brandan M.E. and Satchler G.R. (1997). The interaction between light heavy-ions and what it tells us. *Phys. Rep.* **285**, 143–243.
27. Chaudhuri A.K. (1986). A density-dependent interaction in the folded alpha-nucleus potential. *Nucl. Phys. A* **449**, 243–250.
28. Basu D.N. (2002). Spontaneous heavy cluster emission rates using microscopic potential. *Phys. Rev. C* **66**, 027601 1–4.
29. Basu D.N. (2003). Role of effective interaction in nuclear disintegration processes. *Phys. Lett. B* **566**, 90–97.
30. Basu D.N. (2003). Folding model analysis of alpha radioactivity. *J. Phys. G: Nucl. Part. Phys.* **29**, 2079–2085.
31. Cook J. (1982). DFPOT—A program for the calculation of double-folded potentials. *Comput. Phys. Commun.* **25**, 125–139.
32. Audi G. and Wapstra A.H. (1995). The 1995 update to the atomic mass evaluation. *Nucl. Phys. A* **595**, 409–480.
33. Atzrott U., Mohr P., Abele H., Hillenmayer C. and Staudt G. (1996). Uniform α-nucleus potential in a wide range of masses and energies. *Phys. Rev. C* **53**, 1336–1347.
34. Khoa Dao. T. (2001). α-nucleus optical potential in the double-folding model. *Phys. Rev. C* **63**, 034007 1–15.